Commun Nonlinear Sci Numer Simulat 16 (2011) 4408–4421

Contents lists available at ScienceDirect

Commun Nonlinear Sci Numer Simulat

journal homepage: www.elsevier.com/locate/cnsns

A multi-interval Chebyshev collocation approach for the stability of periodic delay systems with discontinuities

Firas A. Khasawneh [a,*], Brian P. Mann [a], Eric A. Butcher [b]

[a] Department of Mechanical Engineering and Materials Science, Duke University Durham, NC 27708, United States
[b] Department of Mechanical and Aerospace Engineering, New Mexico State University, Las Cruces, NM 88003, United States

ARTICLE INFO

Article history:
Received 12 August 2010
Received in revised form 17 March 2011
Accepted 17 March 2011
Available online 9 April 2011

Keywords:
Chebyshev collocation
Multi-domain
Multi-interval

ABSTRACT

This paper investigates the stability of periodic delay systems with non-smooth coefficients using a multi-interval Chebyshev collocation approach (MIC). In this approach, each piecewise continuous interval is expanded in a Chebyshev basis of the first order. The boundaries of these intervals are placed at the points of discontinuity to recover the fast convergence properties of spectral methods. Stability is examined for a set of case studies that contain the complexities of periodic coefficients, delays and discontinuities. The new approach is also compared to the conventional Chebyshev collocation method.

1. Introduction

Spectral methods are higher-order numerical techniques for solving differential equations. These equations can be ordinary differential equations (ODE), either autonomous or non-autonomous, and/or partial differential equations (PDE) [1,2]. Some application areas include fluid mechanics [3], heat transfer [4], and dynamics [5]. Spectral methods typically employ a global approximation of the solution as a linear combination of smooth basis functions.

Chebyshev polynomials of the first or second kind are one of the basis functions commonly used [6–8]. A series expansion using these polynomials can be used to give accurate approximations while reducing the Runge phenomenon associated with high order interpolants [9]. Another advantage of Chebyshev series is their uniform convergence [10] and the availability of formulas for their manipulation [11]. Although the method of expansion in Chebyshev polynomials has been used for solving ordinary differential equations since at least the 1950s [12], only recently was it adapted in matrix/vector form specifically for ordinary differential equations with periodic coefficients [13]. In addition to solving ODEs and PDEs, Chebyshev spectral methods have been used in the stability analysis of ODEs [14] and delay-differential equations [15,16].

Delay-differential equations (DDEs) are of particular interest in many scientific fields. For example, the Chebyshev expansion method was used in the early work on periodic time-delayed systems [16–18]. This method directly expanded the state in terms of Chebyshev polynomials with unknown coefficients to be determined. In contrast, the Chebyshev-collocation method, which is another method for periodic delays systems, expands the state as an unknown list of values at the Chebyshev–Gauss–Lobatto points. Although the Chebyshev-collocation approach is related to the Chebyshev expansion method at a fundamental level, the former has experienced a quite separate history that parallels the Chebyshev expansion method. For example, the Chebyshev-collocation approach was applied to continuous systems such as beams and plates, see Ref. [19] for a summary.

* Corresponding author.
E-mail addresses: firas.khasawneh@duke.edu, fak7@duke.edu (F.A. Khasawneh).

1007-5704/$ - see front matter © 2011 Elsevier B.V. All rights reserved.
doi:10.1016/j.cnsns.2011.03.025

In time delay systems, the Chebyshev-collocation technique and Floquet theory can be used to determine the stability of autonomous and time-periodic DDEs which appear in control problems [17,18] and machining equations [20]. Computable uniform error bounds for the Chebyshev-collocation method are also available [21], and a sketch of an *a priori* proof for the method's convergence is given in Ref. [22]. The general form of the state-space equations studied by the conventional Chebyshev-collocation method is

$$\dot{\mathbf{y}} = \mathbf{A}(t)\mathbf{y} + \mathbf{B}(t)\mathbf{y}(t-\tau), \tag{1}$$

where τ is the time delay, while $\mathbf{A}(t+T) = \mathbf{A}(t)$ and $\mathbf{B}(t+T) = \mathbf{B}(t)$ are smooth, time periodic coefficients. This method works well and spectral convergence is obtained only when the coefficients are smooth over the entire period. However, abrupt changes, or discontinuities, are sometimes inevitable in physical systems [23,24]. For instance, a periodic DDE with a finite number J of discontinuities in the coefficients can be described by the state-space equation

$$\dot{\mathbf{y}} = \mathbf{A}_j(t)\mathbf{y} + \mathbf{B}_j(t)\mathbf{y}(t-\tau), \quad \text{where } j = 1, 2, \ldots, J, \tag{2}$$

where each $\mathbf{A}_j(t)$ and $\mathbf{B}_j(t)$ represents a continuous function. These discontinuities can cause the rapid convergence property of the conventional Chebyshev collocation approach to be lost [25] which necessitates a different approach to study this class of systems.

Another drawback of typical Chebyshev-collocation methods is the decreased accuracy when severe stretching from the definition domain $[-1,1]$ to the problem domain is encountered [26]. Moreover, the collocation points frequently used are the Chebyshev–Gauss–Lobatto points (CGL); the resolution of these points is improved by increasing the overall order of the method but there is no accurate control of the actual points placement.

Recent studies have overcome the above shortcomings of the typical Chebyshev-collocation method through discretizing the problem domain into multiple sub-domains [27]. Within each sub-domain, Chebyshev series are used to approximate the solution and the different domains are then connected through suitable conditions at the boundaries of any two adjacent intervals, also called inter-boundary conditions. This technique is typically called multi-domain Chebyshev collocation (MDSC) [28] in the context of spatial discretization while for temporal discretization the term multi-interval Chebyshev method is used [25]. The same technique has been recently extended to delay differential equations with multiple and distributed delays [29,30].

This paper extends the multi-interval Chebyshev collocation (MIC) approach to study the stability of periodic DDEs with piecewise-continuous coefficients. The approximate characteristic multipliers, or eigenvalues, of the monodromy operator are calculated and Floquet theory is used to determine stability. In contrast to the typical Chebyshev-collocation method, the current approach gives control over mesh refinement (independent of the order used), reduces errors associated with domain stretching, preserves spectral convergence properties, and accommodates the discontinuities in the coefficients via suitable inter-boundaries placement. In addition, whereas the typical Chebyshev-collocation technique only relies on order-based refinement, or p-type refinement, to achieve convergence, the current approach offers an additional tool to accelerate convergence through interval refinement, or h-refinement.

The organization of the paper is as follows. Section 2 reviews the basics of Chebyshev interpolation and provides the link between the Chebyshev interpolation theory and the Chebyshev collocation method for stability investigations. Section 3 summarizes the conventional Chebyshev-collocation approach for stability determination of DDEs and reports some stability diagrams for a periodic DDE with smooth coefficients. Section 4 expands upon Section 3 and it describes the MIC approach for periodic DDEs with non-smooth coefficients. Section 5 provides case studies for various DDEs with different discontinuities in the coefficients and compares some of the time series obtained from MIC with numerical integration. Section 6 compares the conventional Chebyshev collocation method and the MIC approach while Section 7 provides a discussion of the results and draws conclusions.

2. Interpolation with Chebyshev polynomials

Assume that a function $f(z)$ is continuous over the interval $[-1,1]$, then by the Weierstrass theorem, there exists a polynomial that uniformly approximates f with any desired accuracy. One way to derive the interpolating polynomial is to expand f in a series of smooth basis functions, T_n, according to

$$f(z) = \sum_{n=0}^{N} a_n T_n(z), \tag{3}$$

where a_n are coefficients to be determined. If the basis functions used are the Chebyshev polynomials of the first kind, Eq. (3) becomes the Chebyshev series expansion of f where the Chebyshev polynomials are defined by

$$T_n(z) = \cos(n\cos^{-1}(z)) \quad \text{where} \quad z \in [-1,1]. \tag{4}$$

Although f was assumed to take values in $[-1,1]$, the shifting to any arbitrary period $z : [-1,1] \to \tilde{z} : [a,b]$ can be accomplished through the change of variables

$$\tilde{z} = \frac{1}{2}((b-a)z + a + b). \tag{5}$$

Although it may not be obvious, each T_n in Eq. (4) represents a polynomial in z. This can be seen by calculating the first two Chebyshev polynomials as

$$T_0(z) = 1, \tag{6a}$$
$$T_1(z) = z \tag{6b}$$

and then using the recurrence relationship

$$T_{n+1}(z) = 2zT_n(z) - T_{n-1}(z) \tag{7}$$

to calculate the subsequent polynomials in the Chebyshev series.

A fundamental result is that interpolating at the Chebyshev collocation, or extreme, points minimizes the approximation error in Eq. (3). These collocation points are found from

$$z_n = \cos\frac{n\pi}{N} \quad \text{where } n = 0, 1, \ldots, N, \tag{8}$$

and the change of variables in Eq. (5) can be used to shift these points from $[-1,1]$ to any other interval. Therefore, by evaluating Eq. (3) at the $N+1$ collocation points, a sufficient number of equations is obtained to solve for the unknown coefficients according to

$$\begin{bmatrix} f(z_0) \\ f(z_1) \\ \vdots \\ f(z_N) \end{bmatrix} = \begin{bmatrix} T_0(z_0) & T_1(z_0) & \ldots & T_N(z_0) \\ T_0(z_1) & T_1(z_1) & \ldots & T_N(z_1) \\ \vdots & \vdots & \ddots & \vdots \\ T_0(z_N) & T_1(z_N) & \ldots & T_N(z_N) \end{bmatrix} \begin{bmatrix} a_0 \\ a_1 \\ \vdots \\ a_N \end{bmatrix}. \tag{9}$$

or in matrix form,

$$\mathbf{m} = \mathbf{Q}\,\mathbf{a}, \tag{10}$$

where $\mathbf{m}$ is a vector containing the values of f evaluated at the collocation points. Finding an expression for a_n in terms of the values of f at the collocation points is simplified using the discrete orthogonality relation

$$q_{ij} = \sum_{k=0}^{N} T_i(x_k)T_j(x_k) = \begin{cases} N & \text{for } i = j = 0, \\ \frac{1}{2}N\delta_{ij} & \text{otherwise}, \end{cases} \tag{11}$$

where δ_{ij} is the Kronecker delta function. The expression for the expansion coefficients in terms of the function values at the collocation points becomes

$$\mathbf{a} = \mathbf{Q}^{-1}\mathbf{m}, \tag{12}$$

where the entries of the vector $\mathbf{a}$ are given by

$$a_i = \frac{2}{N\bar{c}_i}\sum_{n=0}^{N}\frac{f(z_n)}{\bar{c}_n}T_i(z_n), \tag{13}$$

and $\bar{c}_{[\cdot]} = 2$ if $[\cdot] = 0$ or $[\cdot] = N$, and is *1* otherwise. Eqs. (13) and (3) can then be combined to give an approximation of f using its values at the collocation points.

An approximation for the first derivative of f with respect to z can be obtained by differentiating Eq. (3) which gives

$$f'(z) = \sum_{n=0}^{N} a_n T'_n(z). \tag{14}$$

However, the recursion relations for the derivative of the Chebyshev functions in terms of the undifferentiated basis coefficients are given by [31,32]

$$T_n(z) = \frac{1}{4}\left[\frac{r_n}{n+1}T'_{n+1}(z) - \frac{d_{n-2}}{n-1}T'_{n-1}(z)\right], \tag{15}$$

where $r_0 = 2$ and $r_n = 1$ for $n \geqslant 0$ but 0 otherwise, and $d_n = 1$ for $n \geqslant 0$ but 0 otherwise. Eq. (15) can be used to define a matrix operator between the differentiated and the undifferentiated Chebyshev basis according to

$$\mathbf{T}'(z) = \mathbf{L}\mathbf{T}(z), \tag{16}$$

where $\mathbf{T}$ is the $N+1$ column vector of the Chebyshev polynomials and $\mathbf{L}$ is the $(N+1)\times(N+1)$ differentiation operational matrix of Chebyshev polynomials [33]. Inserting Eq. (16) into Eq. (14) evaluated at the $N+1$ collocation points yields

$$\mathbf{m}' = \mathbf{D}\mathbf{m}, \tag{17}$$

where $\mathbf{m}'$ is the vector containing the derivative of f evaluated at the collocation points and $\mathbf{D}$ is a spectral differentiation matrix defined on $[-1,1]$ [31,33,34]. The dimension of $\mathbf{D}$ is $(N+1)\times(N+1)$ and its entries are given by

$$D_{00} = -D_{NN} = \frac{2N^2+1}{6}, \tag{18a}$$

$$D_{kk} = \frac{-z_k}{2(1-z_k^2)}, \quad k = 1,\ldots,N-1, \tag{18b}$$

$$D_{kn} = \frac{-\bar{c}_k(-1)^{k+n}}{\bar{c}_n(z_k - z_n)}, \quad k \neq n, \quad k,n = 0,\ldots,N, \tag{18c}$$

where $\bar{c}_{[\cdot]}$ are defined as in Eq. (11). To obtain the differentiation matrix entries for an arbitrary period $[a,b]$, the entries defined in Eq. (18) are multiplied by the scaling factor $2/(b-a)$.

The above approximation procedure can be used to determine the stability of DDEs as will be shown in Section 3. Constructing the time series for initial function DDE problems can also be done using iterative mapping as will be shown in the subsequent sections.

3. Stability analysis of DDEs using Chebyshev collocation

In this section, the Chebyshev collocation method is explained by studying the stability of a delayed, damped oscillator governed by Mathieu's equation [35]. This equation is used since it shows the complexity of both periodic coefficients and a time delay. These two components will be modified later to show the effect of discontinuous coefficients as well. The delayed, damped Mathieu's equation (DDME) has been studied using D-subdivision [36,37] combined with the method of Pontryagin [38]. Insperger and Stépán used analytical and semi-discretization approaches [39–41] while Garg et al. [42] used a second order temporal finite element analysis. This problem has also been studied recently by Patel and Mann using state-space temporal finite element analysis (TFEA) [43].

The DDME can be written as

$$\ddot{x}(t) + \kappa\dot{x}(t) + (\delta + \epsilon\cos t)x(t) = bx(t-\tau), \tag{19}$$

where κ is the damping term, δ and ϵ are constants, $\tau = 2\pi$ is the time delay, and b is a factor scaling the influence of the delayed term. In order to proceed with the stability analysis, Eq. (19) is re-written in its state-space form

$$\frac{d}{dt}\begin{bmatrix} x \\ \dot{x} \end{bmatrix} = \begin{bmatrix} 0 & 1 \\ -(\delta+\epsilon\cos t) & -\kappa \end{bmatrix}\begin{bmatrix} x \\ \dot{x} \end{bmatrix} + \begin{bmatrix} 0 & 0 \\ b & 0 \end{bmatrix}\begin{bmatrix} x(t-\tau) \\ \dot{x}(t-\tau) \end{bmatrix}, \tag{20}$$

or equivalently,

$$\dot{\mathbf{y}} = \mathbf{A}(t)\mathbf{y} + \mathbf{B}\mathbf{y}(t-\tau), \tag{21}$$

where $\mathbf{y}$ is the $q\times 1$ state vector and $\mathbf{A}(t)$ and $\mathbf{B}$ are the $q\times q$ system matrices, where $q = 2$ for this example. This system is time periodic with period $T = \tau = 2\pi$ as indicated by the periodic matrix function $\mathbf{A}(t+T) = \mathbf{A}(t)$. Using a Chebyshev discretization scheme and evaluating Eq. (21) or Eq. (1) at the collocation points gives

$$\widehat{\mathbf{D}}\mathbf{m}_{r+1} = \widehat{\mathbf{M}}_A\mathbf{m}_{r+1} + \widehat{\mathbf{M}}_B\mathbf{m}_r, \tag{22}$$

where $\mathbf{m}_{r+1}$ contains the values of $\mathbf{y}(t)$ in the interval $t\in[0,\tau]$ while $\mathbf{m}_r$ contains the values of the initial function $\boldsymbol{\psi}(t) = \mathbf{y}(t-\tau)$ in $t\in[-\tau,0]$ according to

$$\mathbf{m}_{r+1} = \begin{bmatrix} \mathbf{y}(t_0) \\ \mathbf{y}(t_1) \\ \vdots \\ \mathbf{y}(t_N) \end{bmatrix}, \quad \mathbf{m}_r = \begin{bmatrix} \boldsymbol{\psi}(t_0) \\ \boldsymbol{\psi}(t_1) \\ \vdots \\ \boldsymbol{\psi}(t_N) \end{bmatrix}. \tag{23}$$

In order to describe the matrix $\widehat{\mathbf{D}}$, the $q(N+1)$ square differential operator $\mathbb{D}$ is defined first as the Kronecker product $\mathbb{D} = \mathbf{D}\otimes\mathbf{I}_q$, where $\mathbf{D}$ was defined in Eq. (18) and $\mathbf{I}_q$ is an identity matrix. The matrix $\widehat{\mathbf{D}}$ is then a modified version of the spectral differentiation matrix $\mathbb{D}$ with the following changes (*1*) multiplying by $2/\tau$ to account for the shift $[-1,1]\to[0,\tau]$, and (*2*) changing the last q rows to $[\mathbf{I}_q\mathbf{0}_q\ldots\mathbf{0}_q]$ where $\mathbf{0}_q$ and $\mathbf{I}_q$ are $q\times q$ null and identity matrices, respectively. The change in the last q rows of $\widehat{\mathbf{D}}$, (and the last q rows of $\widehat{\mathbf{M}}_A$ and $\widehat{\mathbf{M}}_B$ as will be shown shortly), is necessary to enforce the periodicity condition which, for this particular case, implies that the states are equal at the end of one period and the beginning of the subsequent one.

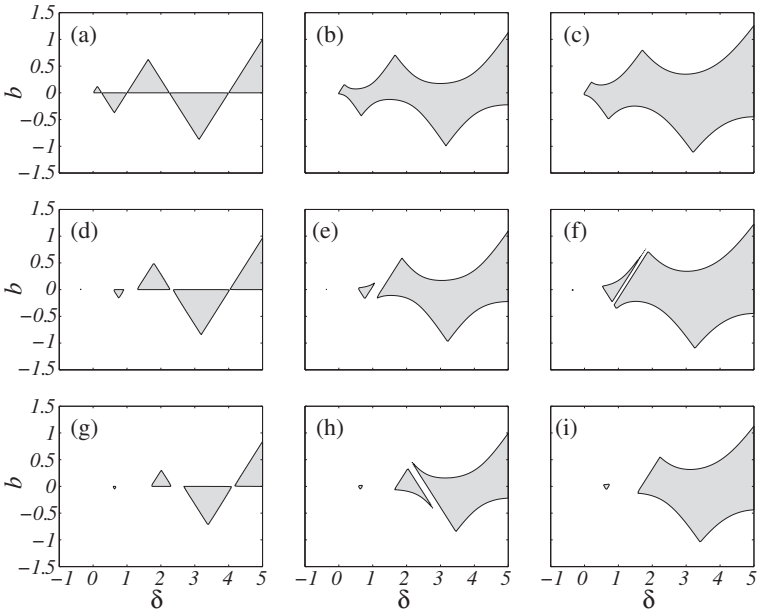

Fig. 1. Stability chart for Eq. (19) using $\tau = 2\pi$, 15 collocation points, and a 200×200 grid. Shaded regions are stable while unshaded regions are unstable. To generate the graphs, the values $\epsilon = 0$, 1 and 2 were used in the 1st, 2nd and 3rd rows, respectively, while $\kappa = 0$, 0.1, and 0.2 in the 1st, 2nd and 3rd columns, respectively.

The $q(N+1)$ square matrix $\widehat{\mathbf{M}}_A$ has the entries

$$\widehat{\mathbf{M}}_A = \begin{bmatrix} \mathbf{A}(t_0) & & & & \\ & \mathbf{A}(t_1) & & & \\ & & \ddots & & \\ & & & \mathbf{A}(t_{N-1}) & \\ \mathbf{0}_q & \mathbf{0}_q & \cdots & \mathbf{0}_q & \mathbf{0}_q \end{bmatrix}, \tag{24}$$

where $\mathbf{A}(t_i)$ is the value of $A(t)$ in Eq. (21) evaluated at the ith collocation point. Similarly, the square $q(N+1)$ matrix, $\widehat{\mathbf{M}}_B$, has the entries

$$\widehat{\mathbf{M}}_B = \begin{bmatrix} \mathbf{B}(t_0) & & & & \\ & \mathbf{B}(t_1) & & & \\ & & \ddots & & \\ & & & \mathbf{B}(t_{N-1}) & \\ \mathbf{0}_q & \cdots & \mathbf{0}_q & \mathbf{0}_q & \mathbf{I}_q \end{bmatrix}, \tag{25}$$

where $\mathbf{B}(t_i)$ is the value of $B(t)$ in Eq. (21) evaluated at the ith collocation point.

Eq. (22) can be rearranged to obtain the dynamic map

$$\mathbf{m}_{r+1} = \mathbf{U}\mathbf{m}_r, \tag{26}$$

where the monodromy matrix $\mathbf{U} = (\widehat{\mathbf{D}} - \widehat{\mathbf{M}}_A)^{-1}\widehat{\mathbf{M}}_B$ is the finite approximation to the infinite-dimensional monodromy operator. The stability of the system described by Eq. (19) can then be determined by examining the eigenvalues of $\mathbf{U}$ using Floquet theory. The asymptotic stability criteria states that the system is stable if all the characteristic multipliers, or eigenvalues, of the monodromy operator are within the unit circle in the complex plane. Alternatively, the inversion of $(\widehat{\mathbf{D}} - \widehat{\mathbf{M}}_A)$ can be avoided by formulating Eq. (22) as a generalized eigenvalue problem, i.e. setting the determinant $|\widehat{\mathbf{M}}_B - \lambda(\widehat{\mathbf{D}} - \widehat{\mathbf{M}}_A)|$ to zero where λ is the characteristic multiplier.

Some stability diagrams for Eq. (19), using different values for δ and κ, are shown in Fig. 1. These results match those obtained with state-space TFEA in Ref. [43].

4. Multi-interval Chebyshev collocation (MIC)

The analysis in Section 3 was for a periodic DDE with smooth coefficients over the entire period. Therefore, a global approximation using a Chebyshev series is justified and the residual error is guaranteed to vanish as the approximation order

is increased. However, many physical applications involve discontinuities in the coefficients during each system period, see Fig. 2. For example, this occurs in milling processes when one of the cutting teeth enters or exits the cut [23]. In this case, the exponential convergence property associated with Chebyshev collocation is lost.

To recover the desired convergence properties, the time of each period is divided into multiple, piecewise-continuous intervals. Inter-boundary points are placed at the points of discontinuities and Chebyshev collocation can then be applied to each subinterval. At the boundaries, the appropriate conditions are enforced to obtain the overall approximation over the full period.

For example, let $t_{p,k}$ be the time at the kth collocation point within the pth interval; assume that $N_p + 1$ is the number of collocation points used within the pth interval and that a total of E subintervals is used in the approximation, i.e. $p \in \{1,2,\ldots,E\}$. The expressions for $\mathbf{m}_{r+1}$ and $\mathbf{m}_r$ then become

$$\mathbf{m}_{r+1} = \begin{bmatrix} \mathbf{y}(t_{1,0}) \\ \mathbf{y}(t_{1,1}) \\ \vdots \\ \mathbf{y}(t_{1,N_1}) = \mathbf{y}(t_{2,0}) \\ \vdots \\ \mathbf{y}(t_{j-1,N_{j-1}}) = \mathbf{y}(t_{j,0}) \\ \vdots \\ \mathbf{y}(t_{E,N_E}) \end{bmatrix}, \quad \mathbf{m}_r = \begin{bmatrix} \boldsymbol{\psi}(t_{1,0}) \\ \boldsymbol{\psi}(t_{1,1}) \\ \vdots \\ \boldsymbol{\psi}(t_{1,N_1}) = \boldsymbol{\psi}(t_{2,0}) \\ \vdots \\ \boldsymbol{\psi}(t_{j-1,N_{j-1}}) = \boldsymbol{\psi}(t_{j,0}) \\ \vdots \\ \boldsymbol{\psi}(t_{E,N_E}) \end{bmatrix}, \tag{27}$$

where the length of both column vectors is given by ℓq where

$$\ell = 1 + \sum_{p=1}^{E} N_p. \tag{28}$$

In contrast to the typical Chebyshev collocation approach, MIC results in overlapping block diagonal matrices. More specifically, let $\widetilde{\mathbb{D}}_p$ be the rectangular $qN_p \times q(N_p + 1)$ matrix obtained by omitting the last q rows of the matrix $\mathbb{D}$ which was described after Eq. (23). A spectral differentiation operator can then be obtained for each element by scaling $\widetilde{\mathbb{D}}$ by $2/h_p$, where h_p is the length of the pth interval. The individual spectral differentiation operators can then be combined in a global differentiation matrix for all the subintervals according to

$$\widehat{\mathbf{D}} = \begin{bmatrix} \left[\frac{2}{h_1}\widetilde{\mathbb{D}}\right] & & & & & & \\ & \left[\frac{2}{h_1}\widetilde{\mathbb{D}}\right] & & & & & \\ & & \ddots & & & & \\ & & & \left[\frac{2}{h_1}\widetilde{\mathbb{D}}\right] & & & \\ & & & & \ddots & & \\ & & & & & \left[\frac{2}{h_1}\widetilde{\mathbb{D}}\right] & \\ \mathbf{I}_q & \ldots & \mathbf{0}_q & \ldots & \mathbf{0}_q & \ldots & \mathbf{0}_q \end{bmatrix}, \tag{29}$$

where $\mathbf{I}_q$ is a $q \times q$ identity matrix with q representing the order of the underlying DDE. Since any two adjacent intervals share a common node, any two subsequent differentiation operators overlap only horizontally by q columns. Further, the last q rows of the global differentiation matrix are padded with the matrix $[\mathbf{I}_q\mathbf{0}_q\ldots\mathbf{0}_q]$ to enforce the continuity condition as was explained after Eq. (22). Hence, the size of the resulting global differentiation matrix is $\ell q \times \ell q$. For example, the resulting global differentiation matrix for $E = 2$, (i.e. using two subintervals), is

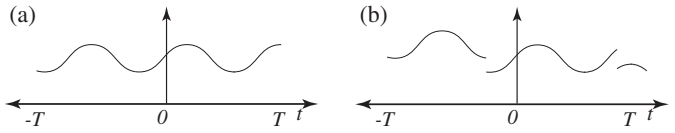

Fig. 2. A representation of the system coefficients over one period. Graph (a) represents smooth coefficients over the full period which allows a global Chebyshev approximation. Graph (b) shows piecewise-continuous coefficients which necessitates a piecewise approximation technique.

$$\hat{\mathbf{D}}|_{E=2} = \begin{bmatrix} \frac{2}{h_1}\begin{bmatrix} D_{0,0}\mathbf{I}_q & \cdots & D_{0,N_1}\mathbf{I}_q \\ \vdots & & \vdots \\ D_{N_1-1,0}\mathbf{I}_q & \cdots & D_{N_1-1,N_1}\mathbf{I}_q \end{bmatrix} & & \\ & \frac{2}{h_2}\begin{bmatrix} D_{0,0}\mathbf{I}_q & \cdots & D_{0,N_2}\mathbf{I}_q \\ \vdots & & \vdots \\ D_{N_2-1,0}\mathbf{I}_q & \cdots & D_{N_2-1,N_2}\mathbf{I}_q \end{bmatrix} \\ \mathbf{I}_q & \cdots & \mathbf{0}_q \quad \cdots \quad \mathbf{0}_q \end{bmatrix} \tag{30}$$

In the MIC approach, the expression for the matrix $\widehat{\mathbf{M}}_{\mathbf{A}}$ reads

$$\hat{\mathbf{M}}_A = \begin{bmatrix} \mathbf{A}(t_{1,0}) & & & & & & & \\ & \ddots & & & & & & \\ & \mathbf{A}(t_{1,N_1}) = \mathbf{A}(t_{2,0}) & & & & & & \\ & & \ddots & & & & & \\ & & \mathbf{A}(t_{p-1,N_{p-1}}) = \mathbf{A}(t_{p,0}) & & & & & \\ & & & \ddots & & & & \\ & & & & \mathbf{A}(t_{E,N_E-1}) & & & \\ \mathbf{0}_q & \mathbf{0}_q & \cdots & & \mathbf{0}_q & \mathbf{0}_q \end{bmatrix}, \tag{31}$$

where the dimension of $\widehat{\mathbf{M}}_{\mathbf{A}}$ is $\ell q \times \ell q$. Similarly, the matrix $\widehat{\mathbf{M}}_B$ has the same dimension as $\widehat{\mathbf{M}}_{\mathbf{A}}$ and it is obtained from

$$\widehat{\mathbf{M}}_B = \begin{bmatrix} \mathbf{B}(t_{1,0}) & & & & & \\ & \ddots & & & & \\ & \mathbf{B}(t_{1,N_1}) = \mathbf{B}(t_{2,0}) & & & & \\ & & \ddots & & & \\ & & \mathbf{B}(t_{p-1,N_{p-1}}) = \mathbf{B}(t_{p,0}) & & & \\ & & & \ddots & & \\ & & & & \mathbf{B}(t_{E,N_E-1}) & \\ \mathbf{0}_q & \mathbf{0}_q & \cdots & & \mathbf{0}_q & \mathbf{I}_q \end{bmatrix}. \tag{32}$$

The global system can then be written as the dynamic map $\mathbf{m}_{r+1} = \mathbf{U}\mathbf{m}_r$ and the stability can be determined by examining the eigenvalues of the monodromy operator, **U**, see Eq. (26). The system is stable if all the eigenvalues of **U** lie within the unit circle in the complex plane.

5. Examples of delayed, time-periodic systems with discontinuous coefficients

The MIC approach allows for the stability investigation of systems with non-smooth coefficients. For example, the discontinuities can be in the periodic term of Eq. (19) indicating a discontinuity in the periodic coefficient. Alternatively, the delay term may include a piecewise continuous gain that can be the result of a piecewise-constant feedback signal.

5.1. Discontinuities in the delay term

A discontinuity in the delay term can be the result of a controller design where the delay feedback can have different gains over different portions of the period. Including this discontinuity in the delay coefficient necessitates a multi-interval

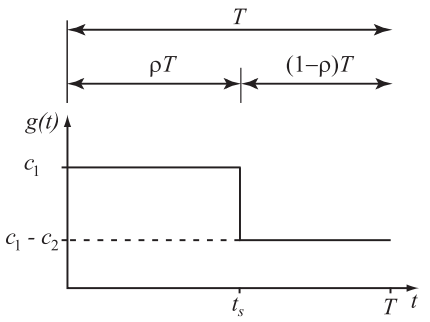

Fig. 3. A plot of the function $g(t)$ described in Eq. (34) over one period.

approach for accurate analysis. For example, consider that Eq. (19) is modified to include a discontinuous feedback gain according to

$$\ddot{x}(t) + \kappa\dot{x}(t) + (\delta + \epsilon\cos(t))x(t) = g(t)x(t-\tau), \tag{33}$$

where κ, δ, and ϵ are constants defined in Eq. (19) while $\tau = 2\pi$ is the time delay. The function $g(t)$ describes the discontinuous nature of the feedback term which can be thought of as an on/off or a piecewise constant delayed feedback. To characterize the switching of the delay term, the fraction $\rho = t_s/T$ can be defined to represent the ratio of the time the gain term

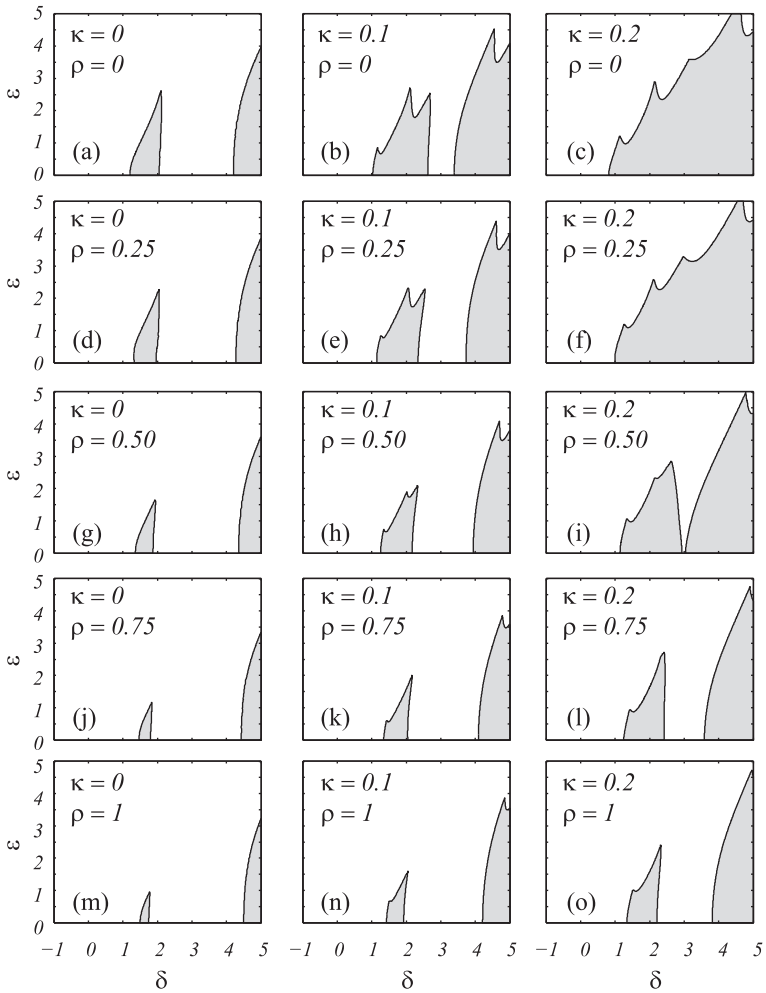

Fig. 4. Stability charts for Eq. (33) using $c_1 = 0.5$, $c_2 = 0.3$, $\tau = 2\pi$ and different values for the parameters κ and ρ. The shaded regions are stable while unshaded regions are unstable. To generate the graphs, two intervals were used with $N_1 = 10$, $N_2 = 12$, and a 200×200 grid.

spends before switching its value to the total length of the period (see Fig. 3). Using this fraction, the function $g(t)$ can be described in terms of the unit step function $u(t)$ as

$$g(t) = c_1 u(t) - c_2 u(t - \rho T), \tag{34}$$

where c_1 and c_2 are constants and the function $g(t)$ is plotted in Fig. 3 over one period.

In the state space form of Eq. (33), the system matrices are given by

$$\mathbf{A}(t) = \begin{bmatrix} 0 & 1 \\ -(\delta + \epsilon\cos(t)) & -\kappa \end{bmatrix}, \quad \mathbf{B}(t) = \begin{bmatrix} 0 & 0 \\ g(t) & 0 \end{bmatrix}. \tag{35}$$

Substituting $c_1 = 0.5$, $c_2 = 0.3$ and using δ and ϵ as the control parameters, the set of stability diagrams in Fig. 4 is obtained for different values of κ and ρ. The cases where $\rho = 0$ and $\rho = 1$ were obtained using the conventional Chebyshev collocation method described in Section 3.

To verify the accuracy of the MIC results, the time series and the phase portrait at the point (2,1) in Fig. 4(b) were obtained from MIC using iterative mapping and compared to numerical integration in Fig. 6(a) and (b), respectively. The solid line in the time series plot of Fig. 6(a) represents the numerical integration results whereas the crosses are obtained from the MIC approach. It can be seen that the results from MIC match the numerical integration results which validates the MIC results. The same observation holds true for the phase portrait plot shown in Fig. 6(b). The initial function used in the comparisons was

$$\psi(t) = \begin{bmatrix} \sin t \\ \cos t \end{bmatrix}, \quad t \in [-T, 0], \tag{36}$$

and the values of the states in the subsequent periods were obtained using iterative mapping.

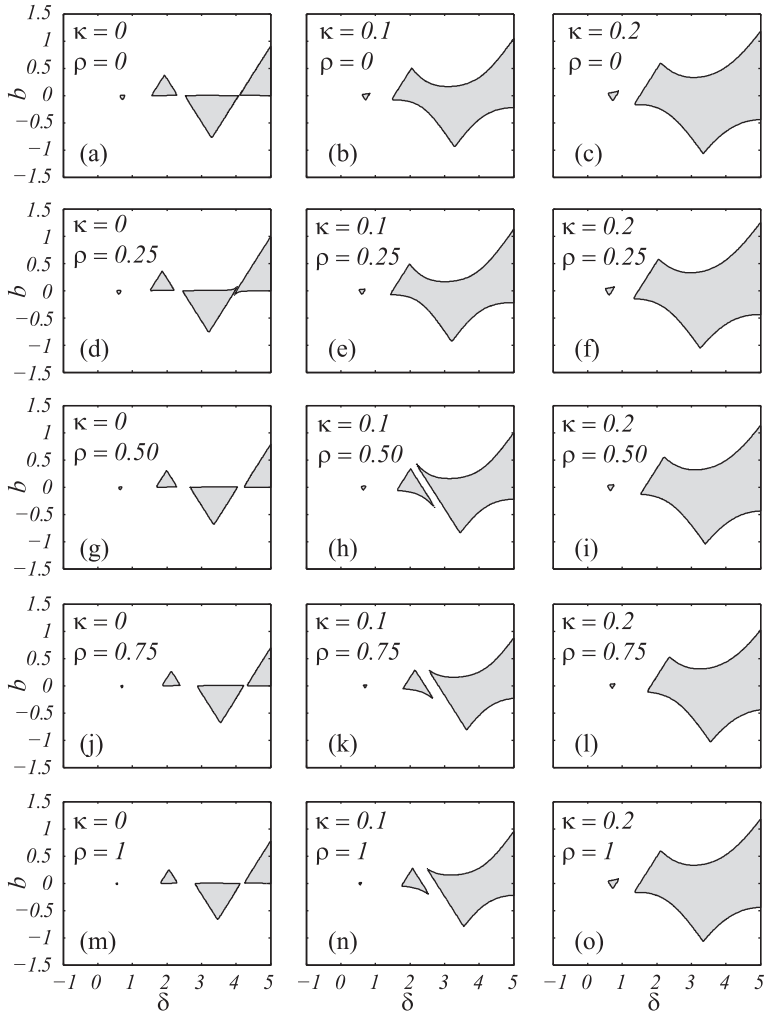

Fig. 5. Stability charts for Eq. (37) using $c_1 = 2.3$, $c_2 = 0.7$, $\tau = 2\pi$ and different values for the parameters κ and ρ. The shaded regions are stable while unshaded regions are unstable. To generate the graphs, two intervals were used with $N_1 = 10$, $N_2 = 12$, and a 200×200 grid.

5.2. Discontinuous parametric periodic excitation

Mechanical systems with rotating components are often modeled as differential equations with parametric excitation. However, if these systems experience intermittent contact [44], the parametric excitation term is typically modified into a piecewise continuous function. Assuming that the contact in the physical model occurs at a certain instance in time during the period and that a delay feedback is applied to the system, the resulting variational equation can be put into the form

$$\ddot{x}(t) + \kappa\dot{x}(t) + (\delta + g(t)\cos(t))x(t) = bx(t-\tau), \tag{37}$$

where κ, δ, and b are constants defined in Eq. (19), $\tau = 2\pi$ is the time delay, and the function $g(t)$ is described in Eq. (34). In the state space form of Eq. (37), the system matrices are given by

$$\mathbf{A}(t) = \begin{bmatrix} 0 & 1 \\ -(\delta + g(t)\cos(t)) & -\kappa \end{bmatrix}, \quad \mathbf{B} = \begin{bmatrix} 0 & 0 \\ b & 0 \end{bmatrix}. \tag{38}$$

Substituting $c_1 = 2.3$, $c_2 = 0.7$ and using δ and ϵ as the control parameters, the set of stability diagrams in Fig. 5 is obtained for different values of κ and ρ. In this figure, the first and last rows corresponding to the cases $\rho = 0$ and $\rho = 1$, respectively, were obtained using the conventional Chebyshev collocation method described in Section 3.

To verify the accuracy of the MIC results, the time series and the phase portrait at the point (4,0) in Fig. 5-k were obtained from MIC using iterative mapping and compared with numerical integration in Fig. 6(c) and (d), respectively. The solid line in the time series plot of Fig. 6(c) represents the numerical integration results whereas the crosses are obtained from the MIC approach. It can be seen that the results from MIC match the numerical integration results which validates the MIC results. The same observation holds true for the phase portrait plot shown in Fig. 6(d). The initial function in Eq. (36) was used in the comparisons.

5.3. Discontinuities in feedback and time periodic terms

Some physical systems exhibit a discontinuous behavior in both the feedback and the time periodic terms [45,46]. In general, the discontinuities in these terms can be different; however, for special types of identical discontinuities, the stability analysis can be simplified as will be shown later. As an example of the general case, consider the equation

$$\ddot{x}(t) + \kappa\dot{x}(t) + (\delta + \epsilon g_1(t)\cos(t))x(t) = bg_2(t)x(t-\tau), \tag{39}$$

where the discontinuities in the time periodic term and the delay term are described by the functions $g_1(t)$ and $g_2(t)$, respectively, according to

$$g_1(t) = c_1u(t) - c_2u(t-\rho_1 T), \tag{40a}$$
$$g_2(t) = c_3u(t) - c_4u(t-\rho_2 T), \tag{40b}$$

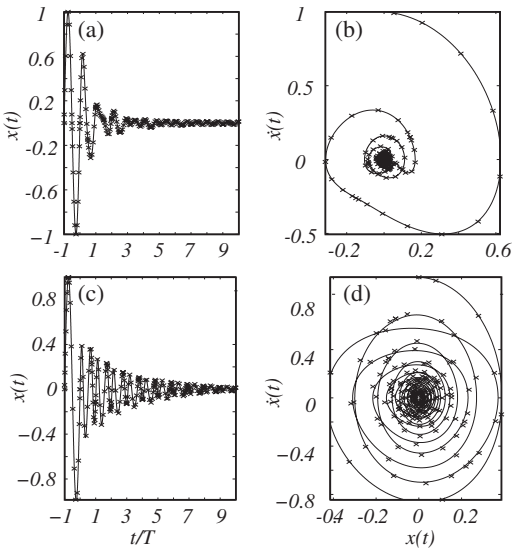

Fig. 6. Comparison between the time series obtained using MIC (crosses) and numerical integration (solid line). The first row corresponds to Fig. 4(b) while the bottom row corresponds to Fig. 5(k).

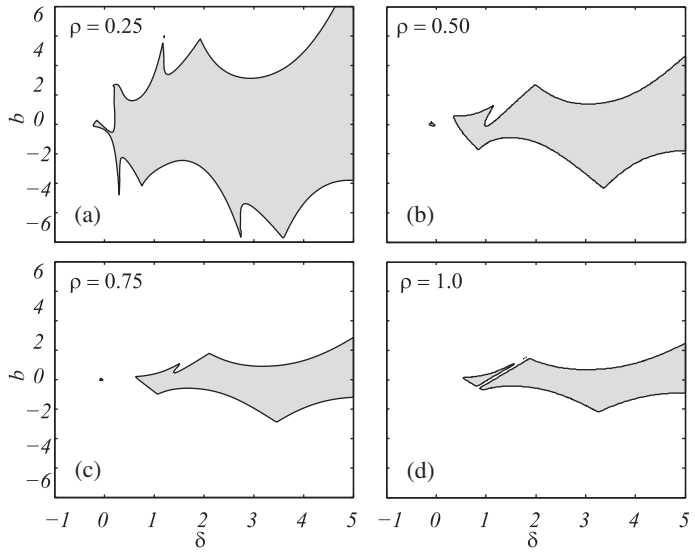

Fig. 7. Stability charts for Eq. (39) using $c_1 = c_2 = 1$, $g_1(t) = g_2(t)$, $\tau = 2\pi$, $\kappa = 0.2$, $\epsilon = 1$, and different values for the parameter ρ. The shaded regions are stable while unshaded regions are unstable. To generate the graphs, one interval was used with $N = 22$, and a 200 $\times$ 300 grid.

where ρ_1 and ρ_2 represent the fraction of T at which the discontinuity occurs in $g_1(t)$ and $g_2(t)$, respectively. Consider the general case where $\rho_1 \neq \rho_2$, to capture the discontinuities in the system, at least a number of subintervals one less than the number of points of discontinuity needs to be used. More specifically, the end points of the intervals are given by the set $\{0, \min(\rho_1 T, \rho_2 T), \max(\rho_1 T, \rho_2 T), T\}$ and if this set includes 4 distinct numbers, then at least 3 subintervals need to be used. Similar to the prior two cases, Eq. (39) can be put into state space form and the MIC approach can be used to find the stability boundaries in the parameter space.

A special case of Eq. (39) is obtained when $c_1 = c_2$ and $g_2(t) = g_1(t)$. This case arises in machining dynamics literature on interrupted turning and milling [20,47] where the parametric excitation and the delay terms are non-zero only over a portion of the period. In this case, although the MIC approach can still be used, a more efficient and accurate approach is to only approximate the portion of the period when these terms are non-zero using Chebyshev collocation. Relating the states of the system when these terms vanish to the states at the beginning of the following period can then be performed using a state transition matrix.

To elaborate, observe that when $g_1(t)$ and $g_2(t)$ both go to zero the resulting equation becomes an unforced linear oscillator with constant coefficients. For this type of system, an exact expression for the state transition matrix can be obtained [46,48]. The resulting forms for the $\widehat{\mathbf{M}}_A$, $\widehat{\mathbf{M}}_B$, and $\widehat{\mathbf{D}}$ matrices are similar to those given in Eq. (22) with one major difference: the continuity condition needs to be changed to account for the vanishing of the parametric excitation and delay feedback by replacing the identity matrix $\mathbf{I}_q$ in the last q rows of $\widehat{\mathbf{M}}_B$ with the $q \times q$ transition matrix $\mathbf{\Phi}$. The expression for the state transition matrix is

$$\mathbf{\Phi} = \frac{1}{\lambda_1 - \lambda_2}\begin{bmatrix} \lambda_1 e^{\lambda_2 t_f} - \lambda_2 e^{\lambda_1 t_f} & e^{\lambda_1 t_f} - e^{\lambda_2 t_f} \\ \lambda_1\lambda_2 e^{\lambda_2 t_f} - \lambda_1\lambda_2 e^{\lambda_1 t_f} & \lambda_1 e^{\lambda_1 t_f} - \lambda_2 e^{\lambda_2 t_f} \end{bmatrix}, \tag{41}$$

where $\lambda_{1,2} = \frac{-\kappa}{2} \pm \frac{i}{2}\sqrt{4\delta - \kappa^2}$, $i = \sqrt{-1}$, and $t_f = (1-\rho)T$ is the duration of time that g_1 and g_2 are switched off [48].

For example, let $c_1 = c_2 = 1$, $g_1(t) = g_2(t)$, $\tau = 2\pi$, $\epsilon = 1$, $\kappa = 0.2$, while δ and b are the control parameters. The resulting stability diagrams for different values of ρ are shown in Fig. 7.

It is important to stress that the above stability analysis is only valid when the time periodic term and the delayed feedback switch on and off and that their switching occurs simultaneously.

6. A comparison between the conventional Chebyshev collocation method and MIC approach

Section 5 showed how the MIC approach can be used to study the stability of different periodic DDEs with discontinuous coefficients. Further, the MIC approach was verified against numerical integration for selected cases of DDEs with non-smooth coefficients. However, the question arises on how the new appraoch compares with the conventional Chebyshev method.

In the context of stability analysis, it is insightful to compare the amplitude of the maximum Floquet multiplier obtained from each method as a function of the number of the collocation points. In the comparisons that follows, the DDE coefficients had one discontinuity, i.e. two intervals were needed for MIC. The order of the approximation in each interval is given by

$N_1 = \lceil N/2 \rceil$ and $N_2 = N - N_1$ where $\lceil \cdot \rceil$ is the ceiling function and N is the approximation order of the conventional Chebyshev method.

For example, consider the case of the periodic DDE described by Eq. (33) and having the parameters $c_1 = 0.5$, $c_2 = 0.3$, $\kappa = 0.1$ and $\rho = 0.5$. The magnitude of the maximum Floquet multiplier, i.e. $\mu = \max(|\lambda|)$, was plotted as a function of N at the point (4.6, 3.75), which lies right inside the stable region, as shown in Fig. 8(a). The results are shown in Fig. 8(c) for the conventional Chebyshev approach (dashed line) and the MIC approach (solid line). It can be seen that the MIC approach converged for $N \approx 40$ where the value of μ remained constant as N was increased. In contrast, for the same values of N, μ fluctuated considerably with the conventional approach as N was varied between odd and even increments.

For $N \geqslant 40$, the Floquet multipliers corresponding to the odd values of N in the conventional approach were almost identical to their MIC counterparts. However, as N increased to an even number, μ jumped to a distant value before matching the MIC result at the next odd increment. This occurs for this specific example since the discontinuity in the feedback coefficient lies in the middle of the interval ($\rho = 0.5$). Specifically, for odd values of N, the conventional Chebyshev mesh has a node at the middle of the interval which could capture the discontinuity and both approaches gave identical results. However, when N is even, the Chebyshev points move away from the center and the conventional approach does not accurately capture the discontinuity which causes the Floquet multiplier to jump. The amplitude of the jump decreases slowly as the mesh becomes more dense and the internal mesh points approach the point of discontinuity. Therefore, whereas in the conventional approach one would increase the number of points and hope that they coincide with the discontinuity, MIC can easily capture the discontinuity by direct placement of the intervals.

As another example, consider the DDE described by Eq. (37) with the parameters $c_1 = 5$, $c_2 = 2.5$, $\kappa = 0.1$ and $\rho = 0.75$. The Floquet multipliers are calculated at the point (2.3, 0.03) shown inside the stability boundary in Fig. 8(b). The convergence plot in Fig. 8(d) shows that the MIC approach converged to a stable multiplier for $N \geqslant 34$. However, the conventional approach gave μ values that jump between different values.

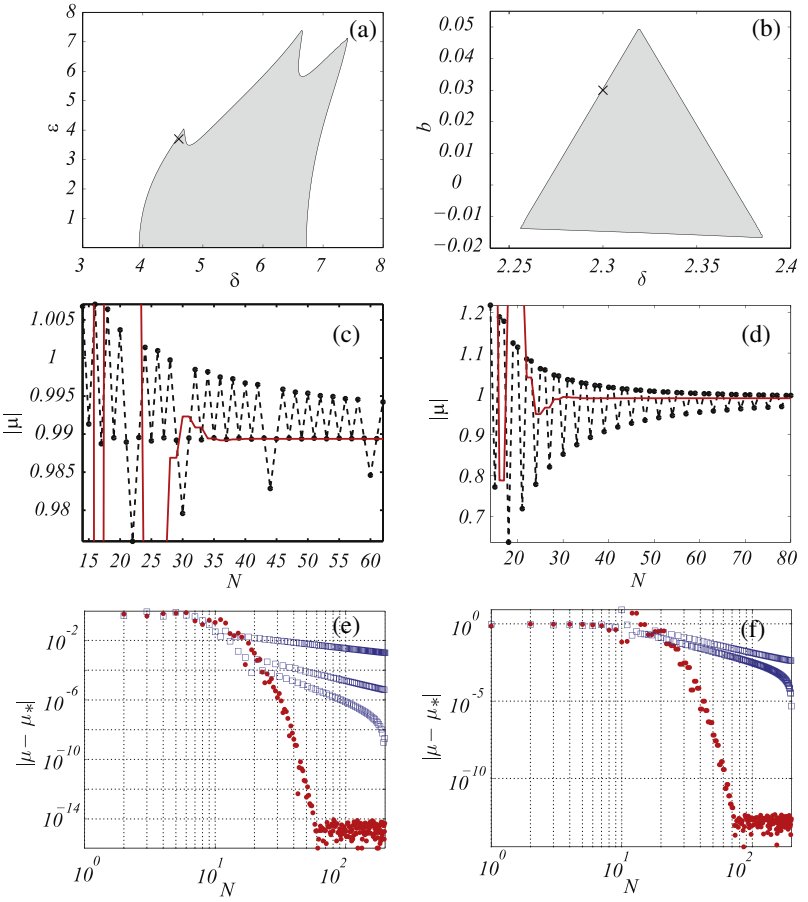

Fig. 8. A comparison between the conventional Chebyshev approach and MIC method. The first column corresponds to Eq. (33) at the point (4.6, 3.75) on the stability diagram. The parameters used are $c_1 = 0.5$, $c_2 = 0.3$, $\kappa = 0.1$ and $\rho = 0.5$. The second column corresponds to Eq. (37) at the point (2.3, 0.03). The parameters used are $c_1 = 5$, $c_2 = 2.5$, $\kappa = 0.1$ and $\rho = 0.75$. The middle row shows the eigenvalues obtained via the conventional approach (dashed) and MIC method (solid) as a function of N. The last row plots the difference $|\mu - \mu_*|$ versus N for MIC (●) and the conventional approach (□).

In contrast to the previous case, the discontinuity did not lie at a point that the conventional mesh could capture. Hence, the Floquet multiplier values fluctuated without matching the MIC results at any point in the shown range. Further, whereas MIC converged to a stable value for μ, the values of μ for the conventional approach fluctuated between the stable and the unstable regimes. The amplitude of the fluctuation decreased as the value of N was increased and the mesh became more dense around the discontinuity. However, only at $N \geqslant 63$ did these fluctuations become small enough to remain within the stable regime. Although the Floquet multipliers oscillated in the stable regime for higher values of N, Fig. 8(d) shows that even for $N = 80$, μ did not reach a convergent value.

To show the loss of the spectral convergence properties in the conventional approach, Fig. 8(e) and (f) plot $|\mu - \mu_*|$ versus N for Eqs. (33) and (37), respectively. The value μ_* is the maximum Floquet multiplier at the maximum N in the used range for the MIC approach, i.e. $\mu_* = \mu(N_{\max})$. From these figures, it can be seen that the spectral convergence property associated with the conventional Chebyshev approach (□) is lost when the DDE contains discontinuous coefficients. On the other hand, the MIC method retains the desired spectral convergence by correctly capturing the discontinuity.

7. Discussion and conclusions

This paper described a multi-interval Chebyshev collocation approach for studying the stability of periodic DDEs with non-smooth coefficients. In contrast to the typical Chebyshev-collocation method, the presented approach gives control over mesh refinement independent of the order used, reduces errors associated with domain stretching, preserves spectral convergence properties, and accommodates the discontinuities in the coefficients via suitable boundary placement.

The MIC approach was described using variants of the delayed, damped Mathieu's equation where the coefficients included discontinuities. Different sets of stability diagrams were reported in Figs. 4, 5 and 7 for the different cases of discontinuous DDEs. The good agreement between MIC and numerical integration was shown in Fig. 6 for two samples of the case studies.

In addition, whereas the typical Chebyshev-collocation technique only relies on order-based refinement, or p-type refinement, to achieve convergence, the current approach offers an additional tool to accelerate convergence through interval refinement, or h-refinement. A comparison between MIC and the conventional Chebyshev approach showed that MIC converged much faster and in a more systematic way than the conventional approach.

In fact, the Floquet multipliers in the conventional approach were shown to fluctuate between the stable and the unstable regimes, even for a large number of collocation points as was shown in Fig. 8(d). However, when the point of discontinuity coincided with a mesh point, the two approaches gave almost identical results as shown in Fig. 8(c) for odd values of N. This indicated that the convergence of the conventional approach is very sensitive to the points distribution and that erroneous results can be obtained—even when the number of collocation points is increased to higher values. This drawback is eliminated in the MIC approach since the location of the discontinuities is captured through suitable element placement and the role of increasing the inner nodes is to obtain spectral convergence. In addition, Fig. 8(e) and (f) show that the MIC approach retains the spectral convergence property whereas this property is lost in the conventional approach.

Therefore, our results indicate that for the case of periodic DDE with non-smooth coefficients the MIC approach is superior to the conventional Chebyshev approach. Specifically, whereas the MIC approach preserves spectral convergence, the conventional approach loses this property and becomes sensitive to the nodes' distribution. Moreover, the MIC approach offers more flexibility in terms of selective mesh refinement as well as exploiting h-convergence properties in addition to the traditional spectral convergence scheme.

Acknowledgments

Support from US National Science Foundation with Grant Nos. CMMI-0900289 and CMMI-0900266 is gratefully acknowledged.

References

[1] Lui SH. Spectral domain embedding for elliptic PDEs in complex domains. J Comput Appl Math 2009;225(2):541–57.
[2] Julien K, Watson M. Efficient multi-dimensional solution of PDEs using Chebyshev spectral methods. J Comput Phys 2009;228(5):1480–503.
[3] Hussaini MY, Zang TA. Spectral methods in fluid dynamics. Ann Rev Fluid Mech 1987;19(1):339–67.
[4] Sun Y, Li B. Chebyshev collocation spectral method for one-dimensional radiative heat transfer in graded index media. Int J Therm Sci 2009;48(4):691–8.
[5] Yagci B, Filiz S, Romero L, Ozdoganlar O. A spectral-Tchebychev technique for solving linear and nonlinear beam equations. J Sound Vib 2009;321(1-2):375–404.
[6] Mason JC, Handscomb DC. Chebyshev polynomials. 1st ed. Chapman & Hall/CRC; 2002.
[7] Leader JJ. Numerical analysis and scientific computation. 1st ed. Addison Wesley; 2004.
[8] Kreyszig E. Advanced engineering mathematics. 9th ed. New York, NY: John Wiley and Sons, Inc.; 2006.
[9] Berrut J, Trefethen LN. Barycentric Lagrange interpolation. SIAM Rev 2004;46(3):501–17.
[10] Johnson LW, Riess RD. On the convergence of polynomials interpolating at the zeroes of $T_n(x)$. Math Z 1970;116(4):355–8.
[11] Barrio R. Algorithms for the integration and derivation of Chebyshev series. Appl Math Comput 2004;150(3):707–17.
[12] Clenshaw C. The numerical solution of linear differential equations in chebyshev series. Proc Camb Philos Soc 1957;53:134–49.
[13] Sinha S, Butcher E. Authors reply to peters, d. a., "some observations on the sinha approach to dynamic response calculations. J Sound Vib 1995;188(4):629–34.
[14] Sinha SC, Wu DH. An efficient computational scheme for the analysis of periodic systems. J Sound Vib 1991;151(1):91–117.

[15] Engelborghs K, Luzyanina T, in 'T Hout KJ, Roose D. Collocation methods for the computation of periodic solutions of delay differential equations. SIAM J Sci Comput 2000;22:1593–609.
[16] Butcher E, Ma H, Bueler E, Averina V, Szabó Z. Stability of linear time-periodic delay-differential equations via Chebyshev polynomials. Int J Numer Methods Eng 2004;59:895–922.
[17] Ma H, Butcher EA, Bueler E. Chebyshev expansion of linear and piecewise linear dynamic systems with time delay and periodic coefficients under control excitations. J Dyn Syst Meas Control 2003;125:236–43.
[18] Deshmukh V, Ma H, Butcher EA. Optimal control of parametrically excited linear delay differential systems via Chebyshev polynomials. Optim Control Appl Methodol 2006;27:123–36.
[19] Trefethen LN. Spectral methods in matlab. Philadelphia: SIAM Press; 2000.
[20] Butcher E, Bobrenkov O, Bueler E, Nindujarla P. Analysis of milling stability by the Chebyshev collocation method: algorithm and optimal stable immersion levels. J Comput Nonlinear Dyn 2009;4(3):031003. doi:10.1115/1.3124088.
[21] Bueler E. Error bounds for approximate eigenvalues of periodic-coefficient linear delay differential equations. SIAM J Numer Anal 2007;45(6):2510–36.
[22] Gilsinn DE, Potra FA. Integral operators and delay differential equations. J Integr Equat Appl 2006;18(6):297–336.
[23] Bobrenkov O, Khasawneh F, Butcher E, Mann B. Analysis of milling dynamics for simultaneously engaged cutting teeth. J Sound Vib 2010;329(5):585–606. doi:10.1016/j.jsv.2009.09.032.
[24] Barton D. Stability calculations for piecewise-smooth delay equations. Int J Bifur Chaos 2009;19(2):639–50. doi:10.1142/S0218127409023263.
[25] Yang B, Zhu Y, Bouaricha A, Phillips J. Applications of the multi-interval Chebyshev collocation method in RF circuit simulation. IEEE Trans Comput-aided Design Integr Circuits Syst 2008;27(3):495–507.
[26] Macaraeg MG, Streett CL. Improvements in spectral collocation discretization through a multiple domain technique. Appl Numer Math 1986;2:95–108.
[27] Orszag S. Spectral methods for problems in complex geometries. J Comput Phys 1980;37:70–92.
[28] Pavoni D. Single and multidomain Chebyshev collocation methods for the korteweg-de vries equation. Calcolo 1988;25(4):311–46.
[29] Breda D, Maset S, Vermiglio R. Pseudospectral differencing methods for characteristic roots of delay differential equations. SIAM J Sci Comput 2005;27(2):482–95.
[30] Breda D, Maset S, Vermiglio R. Numerical computation of characteristic multipliers for linear time periodic coefficients delay differential equations. In: Sixth IFAC workshop on time delay systems TDS2006. L'Aquila – Italy; july 10–12, 2006.
[31] Karageorghis A. A note on the Chebyshev coefficients of the general order derivative of an infinitely differentiable function. J Comput Appl Math 1988;21(1):129–32.
[32] Pfeiffer HP, Kidder LE, Scheel MA, Teukolsky SA. A multidomain spectral method for solving elliptic equations. Comput Phys Commun 2003;152(3):253–73.
[33] Sinha SC, Butcher E. Solution and stability of a set of *p*th order linear differential equations with periodic coefficients via Chebyshev polynomials. Math Probl Eng 1996;2(2):165–90. doi:10.1155/S1024123X96000294.
[34] Dunn D. A Chebyshev differentiation method. Comput Phys Commun 1996;96(1):10–6.
[35] Mathieu E. Memoire sur le mouvement vibratorie d'une membrane de forme elliptique. J Math 1868;13:137–203.
[36] Bellman R, Cooke K. Differential-difference equations. Academic Press Inc.; 1963.
[37] Bhatt SJ, Hsu CS. Stability criteria for second-order dynamical systems with time lag. Appl Mech 1966;33:113–8.
[38] Pontryagin L. On the zeros of some elementary transcendental functions. Izv Akad Nauk SSSR 1942;6:115–34.
[39] Insperger T, Stepan G. Stability chart for the delayed Mathieu equation. Proc R Soc Lon A 2002;458:1989–98.
[40] Insperger T, Stépán G. Updated semi-discretization method for periodic delay-differential equations with discrete delay. Int J Numer Meth 2004;61:117–41.
[41] Insperger T, Stépán G. Semi-discretization of delayed dynamical systems. In: Proceedings of design engineering technical conferences and computers and information in engineering conference, Pittsburgh, Pennsylvania, DETC2001/VIB-21446. ASME; 2001.
[42] Garg NK, Mann BP, Kim NH, Kurdi MH. Stability of a time-delayed system with parametric excitation. J Dyn Syst Meas Control 2007;129:125–35.
[43] Mann B, Khasawneh F. An energy-balance approach for oscillator parameter identification. J Sound Vib 2009;321(1–2):65–78. doi:10.1016/j.jsv.2008.09.036.
[44] Shaw SW, Holmes PJ. A periodically forced piecewise linear oscillator. J Sound Vib 1983;90(1):129–55. doi:10.1016/0022-460(83)90407-8.
[45] Balachandran B. Non-linear dynamics of milling process. Proc R Soc Lon A 2001;359(1781):793–819. doi:10.1098/rsta.2000.0755.
[46] Khasawneh F, Mann B, Insperger T, Stépán G. Increased stability of low-speed turning through a distributed force and continuous delay model. J Comput Nonlinear Dyn 2009;4(4):041003.
[47] Bayly PV, Halley JE, Mann BP, Davis MA. Stability of interrupted cutting by temporal finite element analysis. J Manuf Sci Eng 2003;125:220–5.
[48] Mann BP, Young KA. An empirical approach for delayed oscillator stability and parametric identification. Proc R Soc A 2006;462:2145–60.